DTP/99/114
DAMTP-1999-179
Cavendish-HEP-99/19

BFKL Dynamics at Hadron Colliders

Carlo Ewerz[a,b,1], **Lynne H. Orr**[c,2], **W. James Stirling**[d,e,3] **and Bryan R. Webber**[a,f,4]

[a] Cavendish Laboratory, Cambridge University, Madingley Road, Cambridge CB3 0HE, UK
[b] DAMTP, Centre for Mathematical Sciences, Cambridge University, Wilberforce Road, Cambridge CB3 0WA, UK
[c] Department of Physics and Astronomy, University of Rochester, Rochester NY 14627-0171, USA
[d] Department of Physics, University of Durham, Durham DH1 3LE, UK
[e] Department of Mathematical Sciences, University of Durham, Durham DH1 3LE, UK
[f] Theory Division, CERN, CH-1211 Geneva 23, Switzerland
[1] email: *carlo@hep.phy.cam.ac.uk*
[2] email: *orr@urhep.pas.rochester.edu*
[3] email: *W.J.Stirling@durham.ac.uk*
[4] email: *webber@hep.phy.cam.ac.uk*

Abstract. Hadron colliders can provide important tests of BFKL 'small-x' dynamics. We discuss two examples of such tests, the inclusive dijet jet cross section at large rapidity separation and the number of associated 'mini-jets' in Higgs boson production.

1. Introduction

There has been considerable interest in recent years in QCD scattering processes in the so-called 'high-energy limit', i.e. processes in which $s \gg |t| \gg \Lambda_{\rm QCD}$. The corresponding cross sections are controlled by BFKL dynamics [1, 2], in which large $\ln(s/|t|)$ logarithms arising from soft and virtual gluon emissions are resummed to all orders in perturbation theory. In the leading logarithm approximation, the energy dependence of the cross section is controlled by the (hard) BFKL pomeron: $\sigma \sim s^\lambda$ with $\lambda = \alpha_s 12 \ln 2/\pi$.

The paradigm BFKL process is deep inelastic scattering at small Bjorken x, for which $t \sim -Q^2$, $s \sim Q^2/x$. Resummation of the leading $\alpha_s \ln(1/x)$ logarithms leads to the characteristic $F_2 \sim x^{-\lambda}$ behaviour for the structure function as $x \to 0$. However it has proved difficult in practice to disentangle BFKL and ordinary DGLAP physics at currently accessible x and Q^2 values. One is then led to consider whether hadron colliders such as the Tevatron and LHC can offer a more definitive test of BFKL small-x dynamics.

It was first pointed out by Mueller and Navelet [3] that production of jet pairs with modest transverse momentum p_T and large rapidity separation Δy at hadron colliders would be a particularly clean environment in which to study BFKL dynamics. At asymptotic separations the subprocess cross section is predicted to increase as $\hat{\sigma}_{jj} \sim \exp(\lambda \Delta y)$.

To understand the special features of BFKL dynamics, it will be essential not only to study such fully inclusive cross sections, but also to investigate the structure of the associated final states. For the large Δy dijet cross section, for example, one expects an increasingly large number of 'mini-jets', with transverse momenta of order p_T, produced in the central region. More generally, one can use BFKL dynamics to predict the expected number of such mini-jets in *any* small-x hard scattering process at hadron colliders.

In this note we discuss two tests of BFKL dynamics at hadron colliders: the inclusive dijet cross section and the associated multiplicity of mini-jets in Higgs production.

2. Dijet cross sections at large rapidity separation

We wish to describe events in hadron collisions containing two jets with relatively small transverse momenta p_{T1}, p_{T2} and large rapidity separation $\Delta y \equiv y_1 - y_2$. Defining $\Delta\phi \equiv |\phi_1 - \phi_2| - \pi$ to be the relative azimuthal angle between the jets, the leading-logarithm BFKL prediction for the (gg) subprocess cross section integrated over $p_{T1}, p_{T2} > p_T$ is

$$\left.\frac{d\hat{\sigma}_{gg}}{d\Delta\phi}\right|_{p_{T1}^2, p_{T2}^2 > p_T^2} = \frac{9\alpha_s^2\pi}{2p_T^2}\,\frac{1}{2\pi}\sum_{n=-\infty}^{+\infty} \exp in\Delta\phi C_n(t)\;, \tag{1}$$

with $t = 3\alpha_s \Delta y/\pi$ and

$$\begin{aligned} C_n(t) &= \frac{1}{2\pi}\int_{-\infty}^{+\infty} \frac{dz}{z^2+\frac{1}{4}}\;\exp\left(2t\chi_n(z)\right)\;, \\ \chi_n(z) &= \mathrm{Re}\left[\psi(1) - \psi\left(\tfrac{1}{2}(1+|n|) + iz\right)\right]\;, \end{aligned} \tag{2}$$

where ψ is the digamma function. The total subprocess cross section, and its corresponding asymptotic behaviour, is then [3]

$$\hat{\sigma}_{gg} = \frac{9\alpha_s^2\pi}{2p_T^2}\,C_0(t)\;, \qquad C_0(t)\;\begin{cases} = 1 & \text{for } \; t = 0 \\ \sim \left[\frac{1}{2}\pi 7\zeta(3)t\right]^{-1/2}\;\exp(4\ln 2\; t) & \text{for } \; t \to \infty \end{cases} \tag{3}$$

from which we see the characteristic BFKL prediction of an exponential increase in the cross section with large Δy. It can also be seen from (1) that the average cosine of the azimuthal angle difference $\Delta\phi$ defined above is proportional to $C_1(t)$. In fact we have

$$\langle \cos\Delta\phi \rangle = \frac{C_1(t)}{C_0(t)} \tag{4}$$

and as we shall see below, this falls off with increasing t.

Unfortunately the increase of $\hat{\sigma}$ with Δy disappears when the subprocess cross section is convoluted with parton distribution functions (pdfs), which decrease with

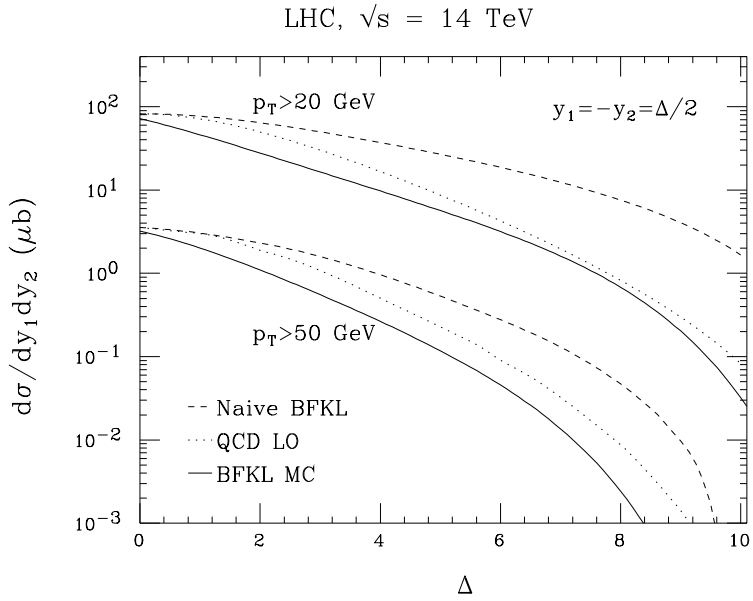

Figure 1. BFKL and asymptotic QCD leading-order dijet production cross sections at the LHC ($\sqrt{s} = 14$ TeV) as a function of the dijet rapidity separation $\Delta \equiv \Delta y$. The three curves at each transverse momentum threshold use: (i) improved BFKL MC with running α_s (solid lines), (ii) leading-order BFKL (dashed lines), and (iii) the asymptotic ($\Delta y \gg 1$) form of QCD leading order (dotted lines).

Δy more rapidly than $\hat{\sigma}$ increases. This is illustrated in fig. 1. The subprocess cross section rise at large Δy becomes a shoulder in the hadron-level cross section, whose exact shape depends on the (large-x) form of the pdfs. To avoid this pdf sensitivity, one can study [4, 5] the *decorrelation* in $\Delta\phi$ that arises from emission of gluons between the jets; BFKL predicts (see eq. (4)) a stronger decorrelation than does fixed-order QCD, and this prediction should be relatively insensitive to the pdfs.

In practice it is not useful to compare analytic asymptotic BFKL predictions directly with experiment because nonleading corrections can be large. In particular, in the analytic BFKL calculation that leads to (1,2) above, gluons can be emitted arbitrarily, with no kinematic cost, and energy and momentum are not conserved. In Ref. [6] (see also [7]) a Monte Carlo approach is used in which the emitted gluons are subject to kinematic constraints (i.e. overall energy and momentum are conserved), and other nonleading effects such as the running of α_s are included. Kinematic constraints are seen to have a significant effect, suppressing the emission of large numbers of energetic gluons. The effect is clearly visible in fig. 1 (solid lines) [8], where the 'improved' BFKL calculation actually gives a *smaller* cross section than that at lowest order. This is due to the sizeable increase in $\hat{s}$, and hence in the large Δy pdf suppression, due to the emitted BFKL gluons.

The azimuthal decorrelation is also weaker in the more realistic BFKL calculation. This is illustrated in fig. 2, where we show [8] the mean value of $\cos\Delta\phi$ in dijet production in the improved BFKL MC approach (upper curves). The jets are completely correlated

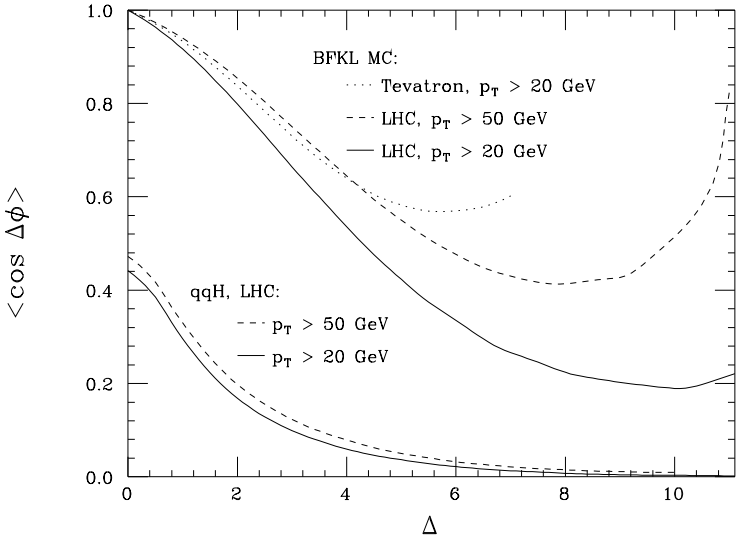

Figure 2. The azimuthal angle decorrelation in dijet production at the Tevatron ($\sqrt{s} = 1.8$ GeV) and LHC ($\sqrt{s} = 14$ TeV) as a function of dijet rapidity difference Δy. The upper curves are computed using the improved BFKL MC with running α_s; they are: (i) Tevatron, $p_T > 20$ GeV (dotted curve), (ii) LHC, $p_T > 20$ GeV (solid curve), and (iii) LHC, $p_T > 50$ GeV (dashed curve). The lower curves are for dijet production in the process $qq \to qqH$ for $p_T > 20$ GeV (solid curve) and $p_T > 50$ GeV (dashed curve).

(i.e. back-to-back in the transverse plane) at $\Delta y = 0$, and as Δy increases we see the characteristic BFKL decorrelation, followed by a flattening out and then an increase in $\langle \cos \Delta\phi \rangle$ as the kinematic limit is approached. Not surprisingly, the kinematic constraints have a much stronger effect when the p_T threshold is set at 50 GeV (dashed curve) than at 20 GeV (solid curve); in the latter case more phase space is available to radiate gluons. We also show for comparison the decorrelation for dijet production at the Tevatron for $p_T > 20$ GeV. There we see that the lower collision energy (1.8 TeV) limits the allowed rapidity difference and substantially suppresses the decorrelation at large Δy. Recent measurements of the dijet decorrelation by the D0 collaboration [9] at the Tevatron are in reasonable agreement with the improved BFKL parton-level predictions. Note that the larger centre-of-mass energy compared to transverse momentum threshold at the LHC would seem to give it a significant advantage as far as observing BFKL effects is concerned.

The lower set of curves in fig. 2 refer to Higgs production via the WW, ZZ fusion process $qq \to qqH$, and are included for comparison [8]. This process automatically provides a 'BFKL-like' dijet sample with large rapidity separation, although evidently the jets are significantly less correlated in azimuthal angle.

3. Associated Jet Multiplicities in Higgs Production at the LHC

One important aspect of the final state at the LHC is the number of mini-jets produced. By mini-jets we mean jets with transverse momenta above some resolution scale $\mu_{\rm R}$ which is very much smaller than the hard process scale Q. Then the mini-jet multiplicity at small x involves not only $\ln x \gg 1$ but also another large logarithm, $T = \ln(Q^2/\mu_{\rm R}^2)$, which needs to be resummed. The results derived in [10, 11] include all terms of the form $(\alpha_{\rm S} \ln x)^n T^m$ where $1 \leq m \leq n$. Terms with $m = n$ are called double-logarithmic (DL) while those with $1 \leq m < n$ give single-logarithmic (SL) corrections. In the calculations the BFKL formalism [1, 2] has been used, but the results are expected to hold [12] also in the CCFM formalism [13, 14, 15, 16] based on angular ordering of gluon emissions.

In order to find $\overline{r}(x)$, the mean number of resolved mini-jets as a function of x, it is convenient to compute first the Mellin transform of this quantity

$$\overline{r}_\omega = \int_0^1 dx\, x^\omega\, \overline{r}(x)\ . \tag{5}$$

We find [11]

$$\overline{r}_\omega = -\frac{1}{\chi'}\left(\frac{1}{\gamma_{\rm L}} + \frac{\chi''}{2\chi'} + \chi\right) T - \frac{1}{2\chi'} T^2 \tag{6}$$

where $\gamma_{\rm L}$ is the Lipatov anomalous dimension which solves

$$\omega = -\bar{\alpha}_{\rm S}\left[2\gamma_{\rm E} + \psi(\gamma) + \psi(1-\gamma)\right] \equiv \bar{\alpha}_{\rm S}\,\chi(\gamma)\ . \tag{7}$$

Here $\bar{\alpha}_{\rm S} = 3\alpha_{\rm S}/\pi$, ψ is the digamma function and $\gamma_{\rm E}$ the Euler constant. In eq. (6), χ' means the derivative of $\chi(\gamma)$ evaluated at $\gamma = \gamma_{\rm L}$. The corresponding expression for the variance in the number of jets, $\sigma_\omega^2 \equiv \overline{r^2}_\omega - \overline{r}_\omega^2$, is more complicated, see [11].

To invert the Mellin transform (5), we can expand eq. (6) perturbatively as a series in $\bar{\alpha}_{\rm S}/\omega$ and then invert term by term using

$$\frac{1}{2\pi i}\int_{\frac{1}{2}-i\infty}^{\frac{1}{2}+i\infty} d\omega\, x^{-\omega-1}\left(\frac{\bar{\alpha}_{\rm S}}{\omega}\right)^n = \frac{\bar{\alpha}_{\rm S}}{x}\frac{\left[\bar{\alpha}_{\rm S}\ln(1/x)\right]^{n-1}}{(n-1)!}\ . \tag{8}$$

The factorial in the denominator makes the resulting series in x-space converge very rapidly. It is then straightforward to compute the mini-jet multiplicity associated with pointlike scattering on the gluonic component of the proton at small x using

$$n(x) = \frac{F(x,Q^2) \otimes \overline{r}(x)}{F(x,Q^2)} \tag{9}$$

where $F(x,Q^2)$ is the gluon structure function and $\otimes$ represents a convolution in x.

As an application of these results, we can compute the mean value N and the dispersion σ_N of the associated (mini-)jet multiplicity in Higgs boson production at the LHC, assuming the dominant production mechanism to be gluon-gluon fusion. At zero rapidity we have gluon momentum fractions $x_1 = x_2 = x = M_H/\sqrt{s}$ where M_H is the Higgs mass, and $N = n(x_1) + n(x_2) = 2n(x)$. Similarly $\sigma_N^2(x) = \sigma_n^2(x_1) + \sigma_n^2(x_2) = 2\sigma_n^2(x)$.

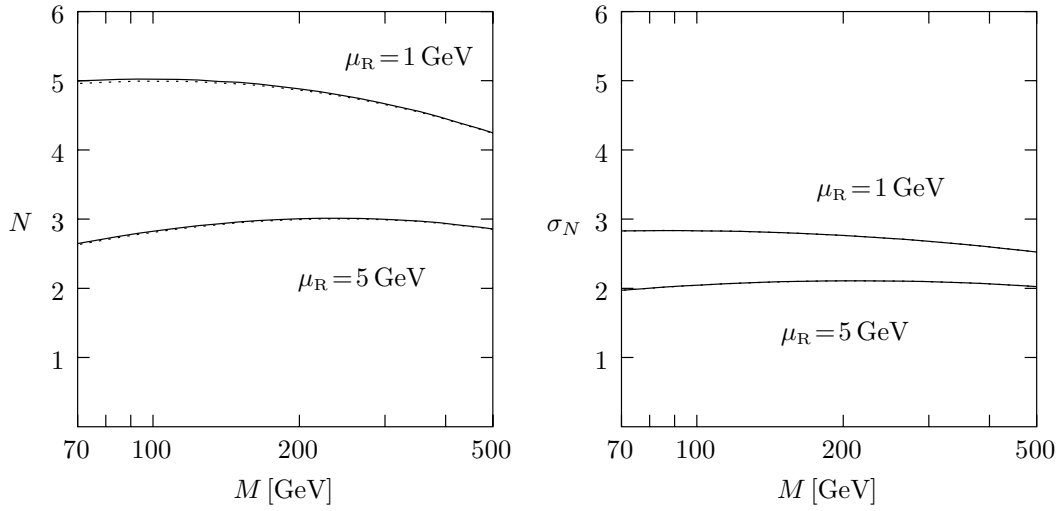

Figure 3. The mean value and dispersion of the number of (mini-)jets in central Higgs production at LHC for two different resolution scales μ_R. Solid lines show the SL results up to the 15th order in perturbation theory, dashed lines correspond to the DL approximation.

The results are shown in fig. 3. We see that in this case the DL results give an excellent approximation and the SL terms are less significant. The mini-jet multiplicity and its dispersion are rather insensitive to the Higgs mass at the energy of the LHC. The mean number of associated mini-jets is fairly low, such that the identification of the Higgs boson should not be seriously affected by them.

References

[1] V.S. Fadin, E.A. Kuraev and L.N. Lipatov, Phys. Lett. **B60**, 50 (1975).
[2] I.I. Balitsky and L.N. Lipatov, Sov. J. Nucl. Phys. **28**, 822 (1978).
[3] A.H. Mueller and H. Navelet, Nucl. Phys. **B282**, 727 (1987).
[4] V. Del Duca and C.R. Schmidt, Phys. Rev. **D49**, 4510 (1994); Phys. Rev. **D51**, 215 (1995); Nucl. Phys. Proc. Suppl. **39BC**, 137 (1995).
[5] W.J. Stirling, Nucl. Phys. **B423**, 56 (1994).
[6] L.H. Orr and W.J. Stirling, Phys. Rev. **D56**, 5875 (1997); Phys. Lett. **B429**, 135 (1998).
[7] C.R. Schmidt, Phys. Rev. Lett. **78**, 4531 (1997).
[8] L.H. Orr and W.J. Stirling, Phys. Lett. **B436**, 372 (1998).
[9] D0 collaboration: S. Abachi *et al.*, Phys. Rev. Lett. **77** 595, (1996).
[10] C. Ewerz and B.R. Webber, JHEP **04**, 022 (1999) hep-ph/9904244.
[11] C. Ewerz and B.R. Webber, JHEP **08**, 019 (1999) hep-ph/9907430.
[12] G.P. Salam, JHEP **03**, 009 (1999) hep-ph/9902324.
[13] M. Ciafaloni, Nucl. Phys. **B296**, 49 (1988).
[14] S. Catani, F. Fiorani and G. Marchesini, Phys. Lett. **B234**, 339 (1990).
[15] S. Catani, F. Fiorani and G. Marchesini, Nucl. Phys. **B336**, 18 (1990).
[16] S. Catani, F. Fiorani, G. Marchesini and G. Oriani, Nucl. Phys. **B361**, 645 (1991).

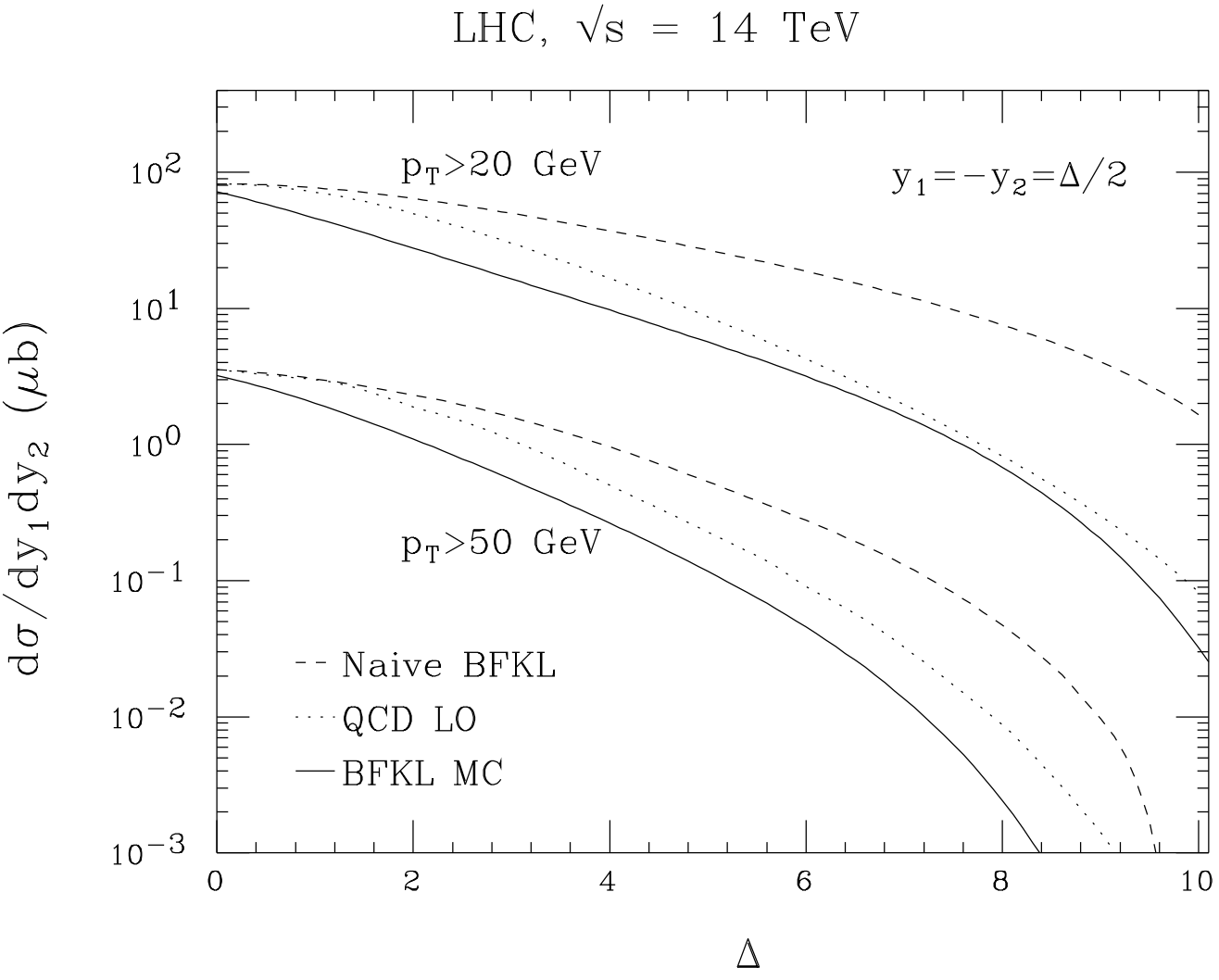
LHC, √s = 14 TeV
p_T>20 GeV
y_1=−y_2=Δ/2
p_T>50 GeV
Naive BFKL
QCD LO
BFKL MC
dσ/dy_1dy_2 (μb)
Δ
10^2
10^1
10^0
10^−1
10^−2
10^−3
0
2
4
6
8
10

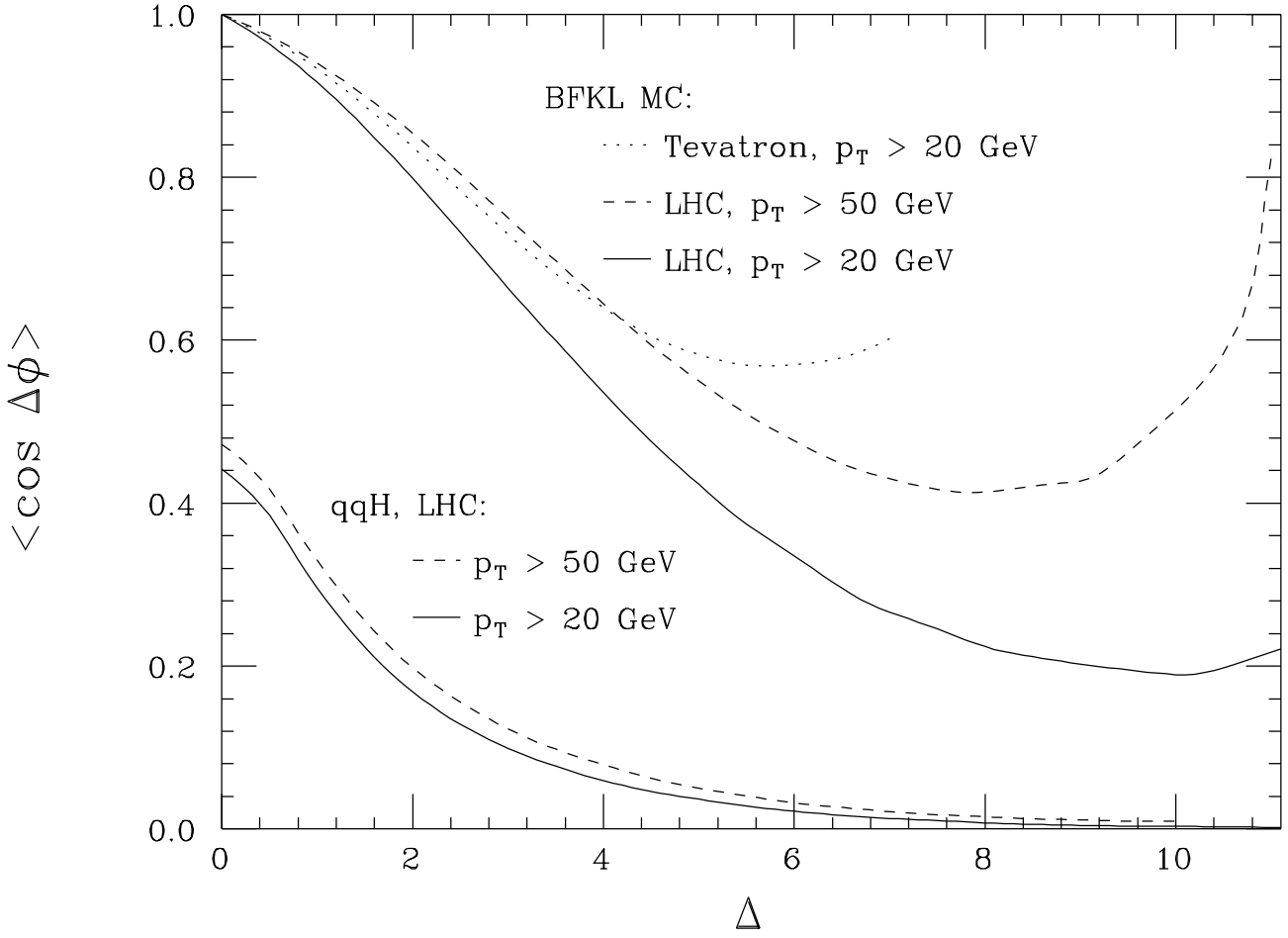
1.0
0.8
0.6
0.4
0.2
0.0
0
2
4
6
8
10
Δ
< cos Δφ >
BFKL MC:
Tevatron, p_T > 20 GeV
LHC, p_T > 50 GeV
LHC, p_T > 20 GeV
qqH, LHC:
p_T > 50 GeV
p_T > 20 GeV